

# J-PARC RCS: HIGH-ORDER FIELD COMPONENTS INHERENT IN THE INJECTION BUMP MAGNETS AND THEIR EFFECTS ON THE CIRCULATING BEAM DURING MULTI-TURN INJECTION

H. Hotchi<sup>#</sup>, H. Harada, and T. Takayanagi

J-PARC Center, Japan Atomic Energy Agency, Tokai, Naka, Ibaraki, 319-1195 Japan

## Abstract

We investigated the cause of residual beam loss during multi-turn injection of the J-PARC 3-GeV rapid cycling synchrotron (RCS). In the RCS, four sets of injection bump magnets (dipole magnets) are employed for multi-turn injection. Numerical simulations considering the actual magnetic field profiles of the injection bump magnets well reproduced empirical beam loss, and pointed that a 3<sup>rd</sup>-order random betatron resonance driven by a sextupole field component inherent in the injection bump magnets is the major source of the beam loss. In this paper, we describe the detailed mechanism of emittance growth and beam loss caused by such a high-order field component of the injection bump magnets including their correction scenario.

## INTRODUCTION

The J-PARC 3-GeV rapid cycling synchrotron (RCS) is the world's highest class of a high-power pulsed proton driver aiming for a 1-MW beam power [1-3].

A 400-MeV H<sup>-</sup> beam from the linac is multi-turn charge-exchange injected to the RCS through a carbon foil over a period of 0.5 ms. The RCS accelerates the injected protons up to 3 GeV with a repetition rate of 25 Hz, providing the high-power beam both to the materials and life science experimental facility (MLF) and the main ring (MR) while switching the beam destination pulse by pulse.

Although the routine RCS beam power is now limited to 500 kW owing to a malfunction of the neutron production target at the MLF, the RCS itself has successfully achieved a 1-MW beam operation with a very fractional beam loss of ~0.25% [3]. The remaining beam loss, which was observed around the injection energy, corresponds to ~333 W. Most of the beam loss was well localized at the collimator section; besides the beam loss power was sufficiently small compared to the capability of the beam collimator system (4 kW). The present situation of beam loss is estimated to be acceptable enough for realizing a routine 1-MW beam operation, but we still have been continuing beam studies aiming for the ultimate beam loss minimization, and also in view of the further beam power ramp-up going beyond 1 MW in the future.

As to the residual beam loss, numerical simulations identified the source; a major part of the residual beam loss comes from high-order field components inherent in four sets of injection bump magnets (pulsed dipole magnets) which are employed for multi-turn injection. The high-order field components, which exist locally in the injection bump magnets not following the RCS's super-periodicity

of 3, have a significant influence on the circulating beam during multi-turn injection via the excitation of high-order random betatron resonances.

In this paper, we discuss the detailed mechanism of beam loss during multi-turn injection, which originates from the high-order field components inherent in the injection bump magnets, and its correction scenario, making use of numerical simulations.

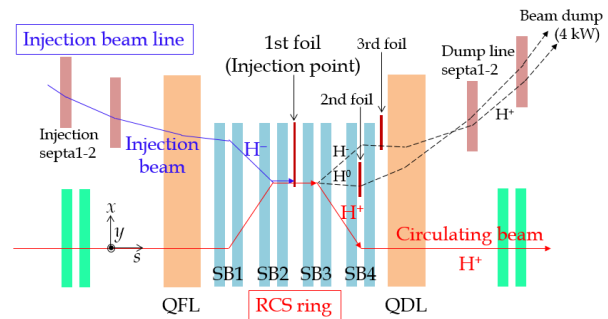


Figure 1: Schematic of the RCS injection section.

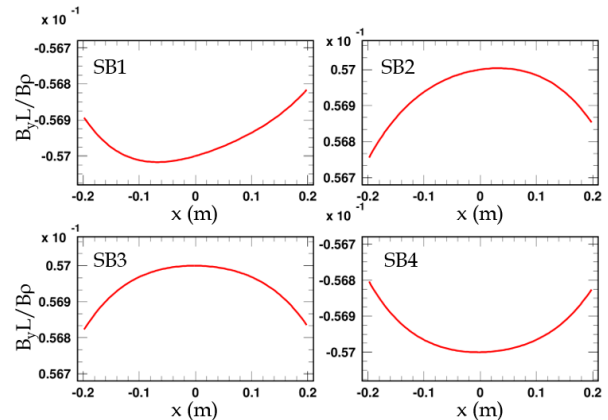


Figure 2: Results of the magnetic field measurements for the SB1-4;  $\int B_y/B_0 ds$  vs.  $x$  at  $y=0$ .

## HIGH-ORDER FIELD COMPONENTS INHERENT IN THE INJECTION BUMP MAGNETS

In the RCS, four sets of same-type pulsed dipole magnets (SB1-4) are utilized for forming an injection orbit bump of  $\Delta x=101$  mm [4], as shown in Fig. 1; they are excited over 0.5 ms (307 turns) during multi-turn injection, and then sharply turned down within 0.35 ms. In this section, the high-order field components inherent in the SBs are discussed with their empirical magnetic field data.

This is a preprint — the final version is published with IOP

<sup>#</sup>hotchi.hideaki@jaea.go.jp

Content from this work may be used under the terms of the CC BY 3.0 licence (© 2019). Any distribution of this work must maintain attribution to the author(s), title of the work, publisher, and DOI

The magnetic field with mid-plane symmetry can be expanded as follows.

$$B_y + jB_x = \sum_{n=0}^{\infty} b_n (x + jy)^n - \frac{b_0''}{2} y^2 \dots \quad (1)$$

Figure 2 shows  $\int B_y/B\rho ds$  for the SB1-4 measured as a function of  $x$  at  $y=0$ . The field profiles reflect the contribution of each  $b_n$  component (pure multipoles) in Eq. (1); each SB includes the  $b_n$  components of at least up to  $n=4$  [5]. Ideally, the SB1-4 generate the same magnetic field distribution except polarity. That is, the SB fields including the high-order field components are cancelled out with each other through the integration over the SB1-4. In such an ideal case, the SB fields have no significant influence on the beam. But, the actual situation is different from that.

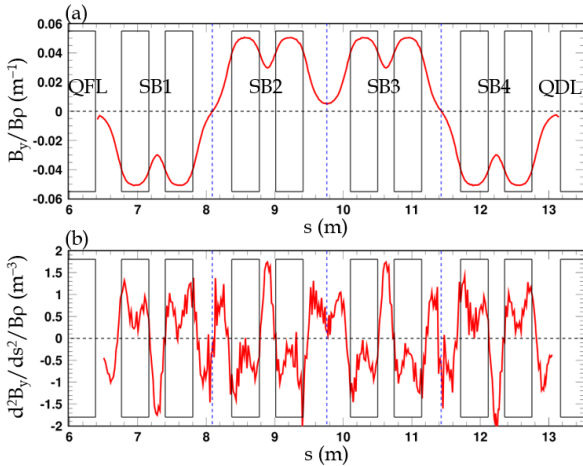


Figure 3: Results of the magnetic field measurements for the SB1-4; (a)  $B_y/B\rho$  vs.  $s$  at  $y=0$  and (b)  $d^2B_y/ds^2/B\rho$  vs.  $s$  at  $y=0$ .

Figure 3 (a) shows  $B_y/B\rho$  measured as a function of  $s$  at  $y=0$ . As shown in the figure, the SB involves a large fringing field because of the large aspect ratio (gap length/core length); besides the SB1-4 are installed closely to each other, where the distance of the SB2-SB3 is different from those of the SB1-SB2 and the SB3-SB4. In addition, the SB1 and the SB4 are close also to the quadrupole magnets (QFL and QDL). Due to such peculiar circumstances, each SB has a different magnetic interference with each neighbouring component. Therefore, the actual field distributions of the SB1-4 are not identical. These facts were confirmed in the magnetic field measurements conducted with a combination of the two magnets such as QFL-SB1, SB1-2, and SB2-3. In addition, the  $x$ -position of the beam is different at each SB while the injection orbit bump is formed, as shown in Fig. 1. Each SB includes significant high-order field components, so different feed-down fields are generated at each SB depending on the position of the beam orbit.

In the actual beam operation, the SB fields are adjusted so that the local orbit bump is closed precisely, namely so that the dipole field component, which the beam feels through the SB1-4, is compensated completely. But, as to

the higher-order field components, such a field compensation is incomplete due to the effects of magnetic interferences and feed-down fields mentioned above. The residual high-order field components, not cancelled out, affect the circulating beam during multi-turn injection.

The second term of Eq. (1), which is the nonlinear field component in proportion to the second order differential of  $b_0$  ( $b_0''=d^2b_0/ds^2$ ), has to be considered as well. As mentioned above, the SB has a large aspect ratio, so that it hardly has a flat field region along the  $s$  axis, as shown in Fig. 3 (a). Accordingly, the second term of Eq. (1) has a non-zero value everywhere, as shown in Fig. 3 (b). Most of the field component is cancelled out through the integration over the SB1-4. But, similarly to the  $b_n$  case, the field compensation is incomplete due to the same reasons. The residual field component, not cancelled out, affects the circulating beam during multi-turn injection.

The strength of each residual  $b_n$  component was evaluated by polynomial least squares fitting ( $n \leq 4$ ) to the field profiles in Fig. 2, in which it was found that the  $b_2$  component (pure sextupole) is the most dominant;  $\int (b_2/B\rho)ds=0.006 \text{ m}^{-2}$ . On the other hand, the strength of the residual  $b_0''$  component was derived from the processing data in Fig. 3 (b);  $1/2 \int (b_0''/B\rho)ds=-0.009 \text{ m}^{-2}$ .

The effect of the  $b_2$  component on the beam is expressed by the following Hamiltonian.

$$\Delta H(x, x', y, y'; s) = \frac{1}{6} \left( \frac{2!b_2}{B\rho} \right) (x^3 - 3xy^2) \quad (2)$$

The first term of Eq. (2) drives the  $3\nu_x = \ell$  and  $\nu_x = \ell$  resonances, while the second term excites the  $\nu_x \pm 2\nu_y = \ell$  resonances. On the other hand, the effect of the  $b_0''$  component is expressed by the following Hamiltonian.

$$\Delta H(x, x', y, y'; s) = -\frac{1}{2} \left( \frac{b_0''}{B\rho} \right) xy^2 \quad (3)$$

The above has a similar form to the second term of Eq. (2), so it also drives the  $\nu_x \pm 2\nu_y = \ell$  resonances.

The effect of each field component on the beam depends on the operational condition (betatron tune, phase advance, etc.) as well as the field strength itself. Thus, it was investigated in detail by numerical simulations assuming the actual operational condition of the RCS.

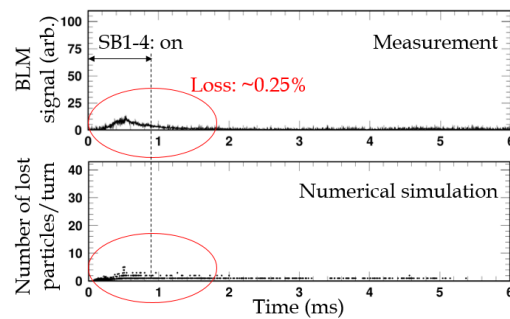


Figure 4: (Upper) Beam loss monitor signal measured at the collimator section. (Lower) Corresponding numerical simulation result.

Content from this work may be used under the terms of the CC BY 3.0 licence (© 2019). Any distribution of this work must maintain attribution to the author(s), title of the work, publisher, and DOI

This is a preprint — the final version is published with IOP

## EFFECTS OF THE SB FIELDS ON THE CIRCULATING BEAM

The numerical simulation including the above  $b_n$  ( $n < 4$ ) and  $b_0''$  components well reproduced the empirical beam loss, as shown in Fig. 4. In this section, we discuss the effects of the SB fields on the circulation beam during multi-turn injection with the numerical simulation result.

Figure 5 shows a 2d plot of the horizontal tune and the horizontal action ( $v_x$  vs.  $2J_x$ ) calculated at the end of injection. In this figure, one can find that beam halo is generated horizontally at  $v_x=6.33$ . As a result of investigating the effects of the  $b_n$  ( $n < 4$ ) and  $b_0''$  components individually, we found that the  $b_2$  component, which is the pure sextupole field component, forms the beam halo via the excitation of the  $3v_x=19$  resonance. The numerical simulation confirmed that this effect of the  $b_2$  component is the major source of the residual beam loss, while the effects of the other  $b_n$  and  $b_0''$  components are not critical in the present operational condition of the RCS.

In order to comprehend what kind of particles suffers the effect of the  $3v_x=19$  resonance more intensely, we looked into the correlation between the beam halo formation and the longitudinal motion of the beam. Figure 6 show the longitudinal phase space ( $s$  vs.  $\Delta p/p$ ) and the tune footprint ( $v_x$  vs.  $v_y$ ) calculated at the end of injection, where the particles painted red correspond to the beam halo particles found in Fig. 5. In Fig. 6 (a), one can find that most of the beam halo particles move around the middle of the longitudinal phase space. The momentum deviations of such particles do not change widely during synchrotron motion, so the turn-by-turn change of their chromatic tune shift is restrictive. In addition, the effects of space charge on such particles are almost constant during synchrotron motion owing to the flat bunch distribution formed by the superposition of a 2<sup>nd</sup> harmonic rf [6,7]. Accordingly, the turn-by-turn change of their space-charge tune shift is also restrictive. That is, the tunes of particles in the middle region of the longitudinal phase space do not change widely turn by turn. As shown in Fig. 6 (b), a part of such particles stays near the  $3v_x=19$  resonance for a relatively long time, and continuously or frequently suffers the effect of the resonance. This is the mechanism of the horizontal beam halo formation observed in Fig. 5.

## CORRECTION SCENARIO

The next subject is to make a scenario for further beam loss mitigation, namely, for minimizing the effect of the  $b_2$  component inherent in the SBs. The most straightforward method is to compensate the driving term of the  $3v_x=19$  resonance with sextupole magnets.

The  $3v_x=19$  resonance is a random resonance driven by the sextupole field errors which exist locally in the SBs not following the super-periodicity of 3. Thus, at least two sets of sextupole magnets connected to individual power supply are required for the purpose. We are now considering the addition of such sextupole correctors for further beam loss mitigation.

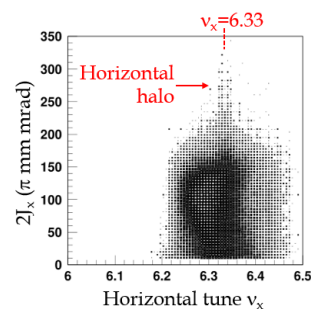


Figure 5: 2d plot of the horizontal tune and the horizontal action calculated at the end of injection.

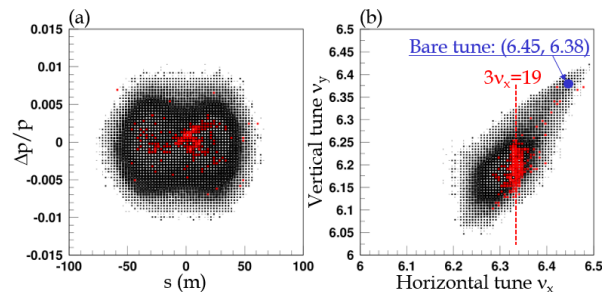


Figure 6: (a) Longitudinal phase space and (b) tune footprint, calculated at the end of injection, where the particles painted red correspond to the beam halo particles found in Fig. 5.

## SUMMARY

We investigated the influences of high-order field components inherent in four sets of injection bump magnets on the circulating beam during multi-turn injection. Ideally, the injection bump fields including the high-order field components are cancelled out with each other through the integration over the four injection bump magnets. But, in the RCS, such a field compensation is incomplete owing to the effects of magnetic interferences and feed-down fields. The resultant residual sextupole field component causes beam halo via the excitation of the 3<sup>rd</sup>-order random resonance, making a beam loss of the order of  $10^{-3}$ . The beam loss is small, but it is not negligible for MW-class high-power machines like the RCS, possibly causing significant machine activations. Now, we discuss the addition of several correction magnets to solve the issue, aiming for the ultimate beam loss minimization.

The multi-turn injection with injection bump magnets is a conventional technique widely employed in high-power proton rings, so the above situation can be a common issue in such facilities. In designing injection bump magnets, the quantitative approaches for possible magnetic interference as well as field quality are essential, and also the pre-arrangement for correction magnets is important as necessary. This is the finding in the present work.

## REFERENCES

- [1] High-intensity Proton Accelerator Project Team, JAERI, Rep. JAERI-Tech 2003-044.

Content from this work may be used under the terms of the CC BY 3.0 licence (© 2019). Any distribution of this work must maintain attribution to the author(s), title of the work, publisher, and DOI

- [2] H. Hotchi *et al.*, *Phys. Rev. ST Accel. Beams* 12, 040402, 2009.
- [3] H. Hotchi *et al.*, *Phys. Rev. Accel. Beams* 20, 060402, 2017.
- [4] T. Takayanagi *et al.*, in *Proc. of the 4th Annual Meeting of Particle Accelerator Society of Japan*, Wako, Japan, 2007, pp. 85–87.
- [5] H. Harada *et al.*, in *Proc. of the 4th Annual Meeting of Particle Accelerator Society of Japan*, Wako, Japan, 2007, pp. 88–90.
- [6] F. Tamura *et al.*, *Phys. Rev. ST Accel. Beams* 12, 041001, 2009.
- [7] H. Hotchi *et al.*, *Phys. Rev. ST Accel. Beams* 15, 040402, 2012.